ELSEVIER

Journal of Nuclear Materials 290–293 (2001) 260–265

journal of nuclear materials

www.elsevier.nl/locate/jnucmat

Assessment of erosion and tritium codeposition in ITER-FEAT

G. Federici [a,*], J.N. Brooks [b,1], D.P. Coster [c], G. Janeschitz [a], A. Kukuskhin [a], A. Loarte [d], H.D. Pacher [e], J. Stober [c], C.H. Wu [d]

[a] *ITER Garching Joint Work Site Co-center, Boltzmannstraße 2, 85748 Garching, Germany*
[b] *Argonne National Laboratory, 9700 S. Cass Ave., Argonne, IL 60439, USA*
[c] *Max-Planck-Institut für Plasmaphysik, 85748 Garching, Germany*
[d] *EFDA, Close Support Unit, Boltzmannstraße 2, 85748 Garching, Germany*
[e] *INRS-Energie et Matériaux, Varennes, Québec J3X 1S2, Canada*

Abstract

Erosion of the first-wall and divertor, and distribution of eroded material in combination with tritium codeposition (primarily with eroded carbon) over many pulses, remain critical issues for the design, operation, and safety of a long-pulse next-step fusion device, such as ITER. These issues are currently being investigated by experiments in tokamaks and in laboratories, as well as by modelling. In this study, we analyse erosion (e.g., by sputtering, ELMs, and off-normal transients) and codeposition effects in the reduced-size ITER device, called 'ITER-FEAT', with a strike-point carbon divertor target and metallic walls, for a 'semi-detached' edge plasma regime using two-dimensional profiles of plasma edge parameters, modelled by the code B2-EIRENE. This paper accompanies the overview paper given by G. Janeschitz et al. [Plasma wall interactions in ITER-FEAT, these Proceedings]. Tritium codeposition with chemically eroded carbon still presents removal/control challenges, albeit to a somewhat lesser extent than in the 1998 ITER design, and demands efficient tritium inventory removal/control techniques. Due to numerous model uncertainties, not the least of which are the plasma solutions themselves, our intent is to provide a scoping analysis, defining trends and suggesting further research needs.

Keywords: ITER; Tritium Inventory; Erosion; Plasma material interaction; Co–deposition; B2/EIRENE

1. Introduction

ITER-FEAT, the next major step in the world fusion program, is designed to have reactor-relevant parameters, i.e., pulsed operation (400 s) at $Q \approx 10$ up to steady-state at $Q \approx 5$, and neutron wall load ≈ 0.5 MW/m^2 [1]. With this long pulse duration and the high duty-cycle desired, the operational availability will be affected by erosion/redeposition of the material of the plasma-facing components (PFCs) and tritium codeposition; erosion requires divertor replacement and codeposition requires tritium removal to control the in-vessel tritium inventory. Further constraints on the PFCs are imposed by disruptions (1–50 MJ/m^2 in 1–10 ms) and Type-I ELM loads ($\leqslant 1$ MJ/m^2 in 0.1–1 ms), the higher values implying melting/ablation for *any* divertor material. Whereas vapour shielding is expected to reduce disruption damage, melt layer loss for metals remains problematic and even concomitant surface heating of nearby components, by radiation from the vapour shield, is severe. The ITER divertor near the strike-points (which bear the majority of disruption and ELM heat loads) has therefore been prudently designed to be clad with carbon. However, the presence of even small carbon areas introduces the need to provide removal techniques to mitigate/control tritium co–deposition.

* Corresponding author. Tel.: +49-89 32994228; fax: +49-89 32994110.
E-mail address: federig@ipp.mpg.de (G. Federici).

[1] US work supported by the US Department of Energy, Office of Fusion Energy.

0022-3115/01/$ - see front matter
PII: S0022-3115(00)00627-9

Previous detailed calculations of erosion/co–deposition were made for the 1998 ITER design [2–4]. The results of new analyses presented here (see also [1]) emphasise the quantification of erosion during the flat-top burn-phase, concentrating on broad trends rather than detailed numbers. Additional issues such as erosion due to ELMs, and off-normal events (e.g., disruptions, VDEs) are only briefly discussed here, and limiter erosion during start-up as well as dust are not treated.

A cross-sectional view of ITER-FEAT is given in Fig. 1, and the main PFC operation parameters are summarised in Table 1. The physics basis, design features and operational aspects of ITER-FEAT are treated in [1]. Beryllium is the primary candidate material for the first-wall, whereas tungsten is the preferred plasma-facing material for the divertor except near the strike plates. There, CFC is chosen because it sublimes rather than melts during disruption thermal quenches and giant ELMs, thereby avoiding generation of surface irregularities that might later form hot spots in normal steady-heat flux operation (for the rationale see [1,4,5]).

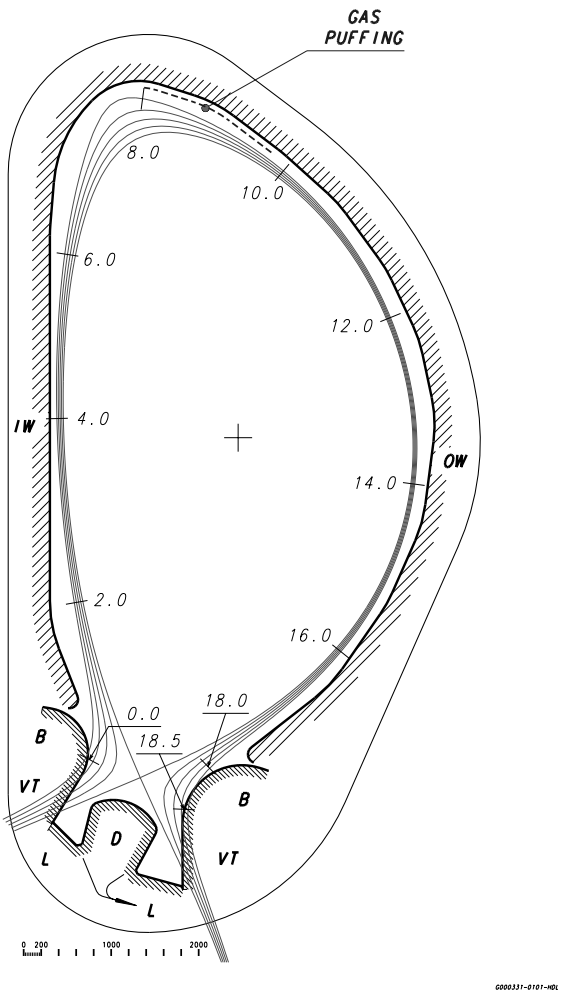

Fig. 1. ITER-FEAT poloidal cross-section showing vacuum vessel (inner contour), divertor vertical target (VT), divertor baffle (B), and divertor private region, consisting of dome (D) liner (L), and inner (IW) and outer (OW) first-wall. Start-up limiters (2 modules) are located at the equatorial level. SOL magnetic surfaces including separatrix are shown (the outermost surface limits the EIRENE calculation grid, numbers are distance in metres along this line).

2. Modelling/calculation methodology

For the calculations, we used the B2-EIRENE [6] plasma solution for a nominal ITER-FEAT case with no impurity seeding, a gas puffing rate of 110 Pa m^3/s, and a separatrix density upstream of 3×10^{19} m^{-3} [7]. For the first-wall and baffle region, erosion occurs due to physical sputtering by charge-exchange (CX) deuterium–tritium (D–T) neutrals from plasma recycling and gas puffing and by D–T and impurity (e.g., He, C) ions which are accelerated in the potential sheath above the sputtering threshold. Fast neutrals from core plasma recombination and from neutral beams (not included here) can also contribute to the formation of the high-energy tail of the neutral distribution. No chemical sputtering and no redeposition of the sputtered material were assumed in the main chamber. To evaluate the neutral fluxes, the EIRENE code was run stand-alone with modifications ensuring accurate computation of the energy spectra of the neutrals impinging upon the surface [8], and the plasma inside the separatrix was assumed to have the specified profiles of temperature and density [9] to provide the correct high-energy tails of CX neutrals. The total CX flux and the mean energy (defined in [8]) along the SOL contour are shown in Fig. 2. Localised gas puffing and recycling at the top of the chamber and strong recycling above the divertor produce the largest fluxes and the lowest E_{mean} there. The net erosion by neutrals was determined by integrating the CX spectra over the angle of incidence and the energy with the sputtering yield. Sputtering erosion by ions was found using the fluxes at the grid edge, temperatures scaled to the wall with 3 cm e-folding length (the B2-EIRENE grid does not reach the wall, Fig. 1), and a Maxwellian distribution function shifted by the sound speed and by acceleration in the assumed Debye potential. Beryllium sputtering yields $Y(E)$ were taken from [10], provided by the VTRIM-3D [11] code, and tungsten yields from the Bohdansky formula [12] with an angle enhancement factor of 2.

Divertor erosion/codeposition including re-deposition in the divertor region was calculated more thoroughly using other codes [3]. Chemical sputtering of carbon by D–T ions, atoms, and molecules, more important here than physical sputtering, is calculated using

Table 1
Design specifications for operation parameters used for the design of the PFCs of ITER-FEAT[a]

	Divertor target	Baffle/dome	First-wall (start-up limiter)
Material	CFC[b] and W	W	Be
Area (m^2)	55 and 60 (liner)	50/30	680 (~10)
No. of replacements	>3	>3	None (for limiter. Tbd)
Normal operation			
Peak surface heat flux (MW/m^2)	10	3	0.5 (~8 for ~100 s)
Peak particle flux ($10^{23}/m^2$ s)	~10	<0.1	0.01 (<0.1)
ELM energy density (MJ/m^2)	<1	Uncertain	
Duration (ms)/{frequency (Hz)}	1/{1–10}		
Off-normal operation	Slow transients	MARFE	
Peak surface heat flux (MW/m^2)	20	~1	
Duration (s)/{frequency (%)}	10 {10}	~10 s	
Disruptions	Thermal quench	Thermal/current quench	
Energy deposition (MJ/m^2)	⩽50	Tbd/uncertainties	
Duration (ms)/{frequency (%)}	1–10 {10}	1–10 {10}	
VDE (full power)[c]			
Energy deposition (MJ/m^2)		<60, uncertainties	
Duration (ms)/{frequency (%)}		0.3/{1}	
Run-away electrons			
Peak surface heat load (MJ/m^2)			~15
Duration (s)/{frequency (%)}			~0.1/{<10}

[a] The pulse duration in ITER-FEAT is about 400 s for a total number of 30 000–40 000 pulses.
[b] Near vertical target strike-points; tungsten elsewhere.
[c] Tbd: to be determined.

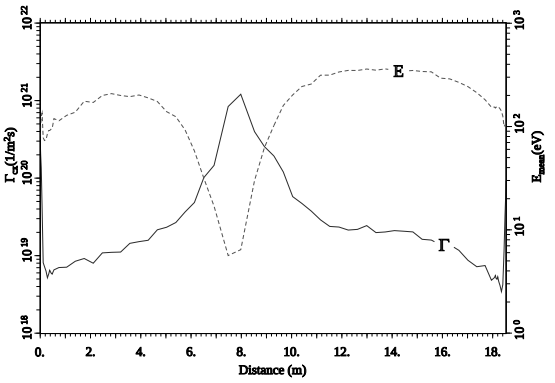

Fig. 2. Total CX flux Γ ($m^{-2} \cdot s^{-1}$) and E_{mean} (eV) vs distance along contour (Fig. 1, divertor at 0.0 and 18.0 m) for $n_e = 3 \times 10^{19}$ m^{-3}.

the yields of [4]. These yields at high fluxes remain uncertain [13], because their determination in plasma experiments is extremely difficult due to uncertainties in plasma parameters, redeposition fractions, and diagnostics interpretation [13,14]. Treatment of erosion/redeposition in the divertor (cf. [3]) in the REDEP/WBC code package [15,16] is improved by (1) use of the full low-energy chemically sputtered hydrocarbon spectrum including methane and higher hydrocarbon emission [17] and rate coefficient package [3,18] and, (2) a new carbon/hydrocarbon reflection model [19] predicting much less reflection (higher sticking) than previously. CX neutral flux and D_2 neutral flux in the divertor were scaled from previous results to show trends.

To calculate tritium codeposition it is assumed that (i) all material not redeposited at the wall goes to the divertor (since ionisation of wall-sputtered material in the SOL and subsequent transport along the field lines is expected), (ii) the redeposited material grows locally (does not erode further), (iii) the D–T flux to the growing surface is large and energetic enough to reach saturation at the temperature-dependent saturated value for C and Be–O [3]. For tungsten no codeposition effect is expected.

3. Results of analyses and discussion

3.1. First-wall erosion

Fig. 3 shows the erosion rate for neutrals and ions along the first-wall for Be and, only for comparison, for W. The beryllium peak erosion rate of ~0.1 nm/s (~0.3 cm/burn-yr) is acceptable for the low duty-factor operation of ITER-FEAT. Tungsten erosion is between one and two orders of magnitude lower. The total Be flux integrated over the entire ITER-FEAT first-wall was

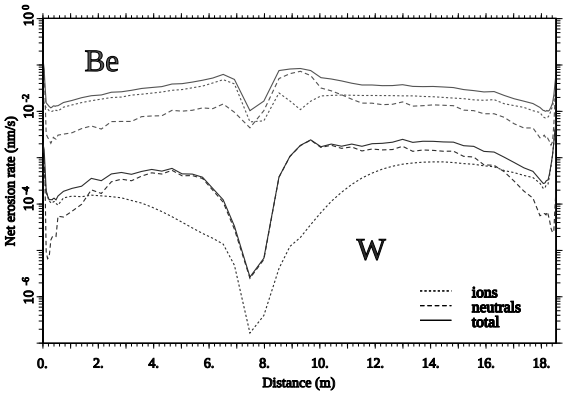

Fig. 3. Sputtered erosion rate in nm/s (from DT neutrals and DT and impurity ions) vs distance along contour (Fig. 1, divertor at 0.0 and 18.0 m) for Be, W.

estimated to be $\sim 4.7 \times 10^{21}$ s^{-1}, whereas the integrated tungsten flux is about two orders of magnitude lower, $\sim 9 \times 10^{19}$ s^{-1}. However, the permissible tungsten impurity flux (limited by the increased radiation from the plasma core) is about three orders of magnitude lower than the permissible flux from light impurities, C and Be (limited by core dilution). The Be codeposition rate, assuming that half of this Be builds up in lower temperature areas ($\leqslant$200°C at the bottom of the divertor target and private region) and using trapping data [3], is estimated to be in a range of 0.1–0.4 g-T/400 s pulse.

3.2. Divertor erosion/codeposition

The calculations, performed using updated models for chemical sputtering and transport and scaling physical sputtering results from the previous design, yield a tritium codeposition rate of ~2 g-T/400 s pulse, about 1/3 the previous value [3,4]. This is for the carbon portion of both divertors with inner divertor results scaled from those for the outer divertor. About one half of this reduction is due to the reduced tokamak size, and the remainder to differences in plasma parameters, surface temperature profile, and changes in the sputtering and hydrocarbon reflection model. Individual contributions to the tritium codeposition rate are about 0.4 and 1.6 g-T/400 s pulse for physical and chemical sputtering, respectively. The peak net erosion rate is 6.4 nm/s (i.e, 2.6 μm/400 s pulse or 20 cm/burn-yr), occurring in the detached portion of the divertor plate, and due almost entirely to chemical sputtering. This compares to a peak of 15.5 nm/s (i.e., 15.5 μm/1000 s pulse or 49 cm/burn-yr) for the 1998 ITER design.

The previous [3] and present analyses are at most reliable for indicating trends, not firm quantitative predictions. The overall REDEP/WBC model is well-validated for attached regimes [20] with carbon, beryllium and tungsten, but not yet for detached plasma regimes. Key outstanding issues of the carbon erosion models (see [3,4]) include the possible flux dependence, if any, of carbon chemical sputtering, very low energy but non-thermal (~1–3 eV) hydrocarbon reflection coefficients, and overall properties of redeposited material.

Once carbon is used, the operational tritium in-vessel inventory limit of a few hundred grams dictates use of tritium control and removal methods (under development but not yet proven, see [4]) to deplete the codeposited layers or to remove them, unless the codeposition surfaces are designed to remain 'hot' during operation, to prevent tritium accumulation. A hot 'transparent tungsten liner' to minimise tritium codeposition (800–1000°C) by de-hydrogenating the carbon and/or recombining the active radicals is also being developed. Preliminary experiments [21] to understand the carbon deposition on the hot-liner and cold structural parts behind it are promising but the possible formation of films behind the liner, by hydrocarbon radicals having a low sticking coefficient, remains preoccupying. The estimates reported here do not include the mitigating effects of a 'hot liner'.

3.3. Erosion during thermal quench disruption and VDEs

The erosion due to the thermal quench of disruptions (1–5 ms) has been assessed by various authors [13,22–24]. ~10 μm is estimated to be the vaporised thickness per disruption for carbon and tungsten, and in addition for tungsten formation of a melt layer of about 100 μm is expected [13]. Longer events such as vertical displacement events (VDE, $\geqslant$100 ms) would cause severe surface melting and erosion and additional damage (e.g., interface bond degradation and coolant tube burnout). The erosion due to VDEs has been modelled [22,25,26], and runaway electron effects on PFCs have been analysed [27]. Vaporisation and melt layer thicknesses for Be, without vapour shielding, produced by VDEs depositing about 20 MJ/m^2 in 100 ms are calculated to be ~140 and 520 μm, respectively (0.2 and 450 μm for tungsten).

3.4. Divertor erosion during ELMs

As ELMs have lower energy densities than disruptions, but are unlikely to produce a vapour shield optically thick enough to radiate away the power deposited and prevent damage, their number must be limited. No complete calculations are presently available below 10 MJ/m^2. 1-D material response calculations are shown in Fig. 4 (assuming no temperature ratcheting) give the number of ELMs to erode a 20 mm thick carbon target and a 10 mm thick tungsten target. If we assume that Type-I ELMs transport ~20% [28,29] of the power

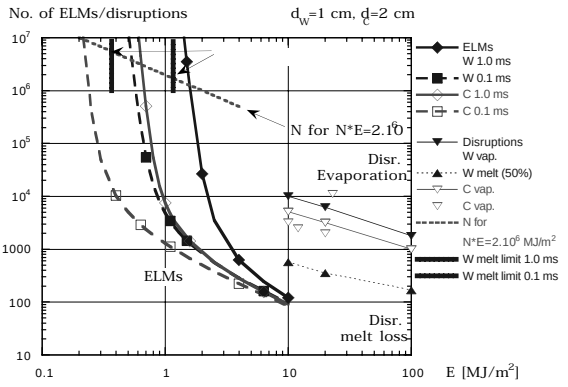

Fig. 4. Number of ELMs N to erode 1 cm of W (solid symbols) or 2 cm of C (hollow symbols) vs ELM energy per unit area E, for ELM duration of 0.1 (lozenges) and 1ms (squares). Melt limit for W indicated. Disruption evaporation and melt loss numbers with vapour shield (cf. Ref. in [2]) also shown. For line $N \times E = 2 \times 10^6$ MJ/m^2 see text.

crossing the separatrix (ELM frequency varies inversely as the ELM energy) that the resulting 18 MW is deposited on 7 m^2, and that the plates are to withstand 2000 shots lasting 400 s, the product of ELM number and energy is $N \times E$ is at least 2×10^6 MJ/m^2. For 0.1–1 ms duration, the resulting maximum allowable ELM energy (see intersection of $N \times E$ with ELM erosion in Fig. 4) is 0.22–0.64 MJ/m^2 for carbon and 0.54–1.6 MJ/m^2 for tungsten. However, tungsten surface melting must be avoided (to allow operation for millions of cycles) so that these values must be reduced to the melt limit, 0.37 and 1.17 MJ/m^2 for tungsten. The values of $E/\sqrt{(t)}$ are about 20 MJ m^{-2} s$^{-0.5}$ for carbon and 37 for tungsten. The former is lower than the value of 40 quoted for carbon in [29] because triatomic carbon clusters and high-temperature material properties are considered here. Note that the expected ELM amplitude according to one Type-I ELMs scaling [28] is 2% of the stored energy, yielding 1.1 MJ/m^2 in ITER-FEAT. Therefore, tungsten would be barely acceptable for ELM durations of 1 ms. Carbon, and also tungsten at ELM durations shorter than 1 ms, require control methods to lower type-I ELM amplitudes. Note also that, because of the steepness of the erosion curves and the requirement of no W melting, even if the number of ELMs could be reduced there, would be little change in the limiting energy density.

4. Uncertainties and future priorities

Because of uncertainties in the modelling and the underlying database, the present results provide trends rather than precise predictions. Further sensitivity studies of edge-plasma conditions and ion impact at the wall are required. Relevant physical processes now ignored [30] must be included. Chemical erosion of carbon, particularly its flux dependence, must be better characterised. Detailed analyses of plasma transported sputtered material, as well as mixed-material effects, are needed. Prudently, new design solutions which do not use carbon are also being explored, with emphasis on tungsten. Shortcomings of tungsten – lack of operational experience and melt layer formation and loss during disruptions – need to be explored. Additionally, disruption control (minimisation of frequency and thermal quench energy deposition) needs to be developed. Under 'normal' or steady-state operating conditions, operation at lower densities may introduce new problems.

5. Conclusions

Keeping in mind the uncertainties summarised above, the main conclusions on erosion/redeposition and codeposition effects for a reference 'semi-detached' plasma edge solution in ITER-FEAT are:

First-wall. Peak erosion, mainly by energetic CX neutrals and impurity ions, of a Be-clad first-wall is estimated to be about 0.1 nm/s, with low redeposition. This rate is acceptable for ITER-FEAT but may be too high for high duty factor reactor operation. The corresponding tritium codeposition rate is 0.1–0.4 g-T/400 s pulse. The erosion of a tungsten-clad wall is calculated to be negligible, but the permitted impurity flux would be three orders of magnitude lower for tungsten than for beryllium.

Divertor. The tritium codeposition rate is estimated at 2 g-T/400 s pulse, about 1/3 of that for the 1998 ITER design. The peak net erosion rate in normal operation is 2.6 μm/400 s pulse, occurs in the detached portion of the divertor plate, and is due almost entirely to chemical sputtering. For the erosion depth by ELMs to be significantly smaller than that by sputtering and to avoid surface melting for ELM durations of 0.1 and 1 ms, the energy density per ELM must remain below 0.22–0.64 MJ/m^2, respectively, for carbon 20 mm thick, or below 0.37 and 1.17 MJ/m^2, respectively, for tungsten 10 mm thick.

Acknowledgements

Useful discussions with A.A. Haasz and J. Roth about erosion yields and the computational support of G. Strohmayer are gratefully acknowledged. This paper was prepared as an account of work undertaken within the framework of the ITER EDA Agreement. The views

and opinions expressed herein do not necessarily reflect those of the Parties to the ITER Agreement, the IAEA or any agency thereof. Dissemination of the information in this paper is governed by the applicable terms of the ITER EDA Agreement.

References

[1] G. Janeschitz et al., Plasma wall interactions in ITER-FEAT, these Proceedings.
[2] H.D. Pacher et al., J. Nucl. Mater. 241–243 (1997) 255.
[3] J.N. Brooks et al., J. Nucl. Mater. 266–269 (1999) 58.
[4] G. Federici et al., J. Nucl. Mater. 266–269 (1999) 14.
[5] V. Barabash et al., Phys. Scripta T81 (1999) 74.
[6] D.P. Coster et al., J. Nucl. Mater. 241–243 (1997) 690.
[7] A. Kukushkin et al., these Proceedings.
[8] H. Verbeek et al., Nucl. Fus. 30 (1998) 1789.
[9] M. Shimada et al., Physics design of ITER-FEAT, Toki Conference, January 2000.
[10] J.N. Brooks, D.N. Ruzic, D.B. Hayden, Fus. Eng. Des. 37 (1997) 455.
[11] D.N. Ruzic, Nucl. Instrum. and Meth. B 47 (1990) 239.
[12] W. Eckstein et al., Sputtering Data, Rep. 9/82, Max-Planck-Inst. für Plasmaphysik, Garching, 1993.
[13] G. Federici et al., Plasma-materials interactions in current tokamaks and their implications for next-step fusion reactors, Nucl. Fus., to appear.
[14] M. Stamp et al., these Proceedings.
[15] J.N. Brooks, Nucl. Tech. Fus. 4 (1983) 33.
[16] J.N. Brooks, Phys. Fluids 8 (1990) 1858.
[17] B.V. Mech, A.A. Haasz, J.W. Davis, J. Nucl. Mater. 255 (1998) 153.
[18] D. Alman, D.N. Ruzic, J.N. Brooks, Physics of Plasmas 7 (2000) 1421.
[19] D. Alman, MS thesis, University of Illinois at Urbana/Champaign, Department of Nuclear, Plasma and Radiological Engineering, May 2000.
[20] J.N. Brooks, D.G. Whyte, Nucl. Fus. 39 (1999) 525.
[21] I. Arkhipov et al., these Proceedings.
[22] A. Hassanein et al., Fus. Eng. Des. 39–40 (1998) 201.
[23] A. Hassanein et al., these Proceedings.
[24] H. Wuerz et al., these Proceedings.
[25] G. Federici, A.R. Raffray, J. Nucl. Mater. 244 (1997) 101.
[26] I. Smid et al., J. Nucl. Mater. 233–237 (1996) 701.
[27] A.R. Raffray et al., Effects of runaway electrons and VDE's on ITER first-wall, in: B. Beaumont et al. (Ed.), Proceedings of the 20th Symposium on Fusion Technology, vol. 1, Marseille, France, 1998, p. 211.
[28] ITER Physics Basis, Nucl. Fus. 39 (1999) 2137.
[29] A.W. Leonard al., J. Nucl. Mater. 266–269 (1999) 109.
[30] P. Coad et al., these Proceedings.